



Development and characterization of a DMAPS chip in TowerJazz 180 nm technology for high radiation environments

Christian Bospin^{a,*}, Ivan Berdalovic^{b,d}, Ivan Caicedo^a, Roberto Cardella^b, Jochen Dingfelder^a, Leyre Flores^b, Tomasz Hemperek^a, Hans Krüger^a, Thanushan Kugathasan^b, Cesar Marin Tobon^b, Konstantinos Moustakas^{a,c}, Heinz Pernegger^b, Francesco Piro^b, Petra Riedler^b, Walter Snoeys^b, Norbert Wermes^a

^a Universität Bonn, Physikalisches Institut, Nußallee 12, 53115 Bonn, Germany

^b CERN, Esp. des Particules 1, 1211 Meyrin, Switzerland

^c Paul Scherrer Institut, Forschungsstrasse 111, 5232 Villigen PSI, Switzerland

^d University of Zagreb, Department of Electronics, Microelectronics, Computing and Intelligent Systems, Unska 3, 10000 Zagreb, Croatia

ARTICLE INFO

Keywords:

Depleted monolithic active pixel sensor
Pixel detectors
Monolithic pixels
MAPS
DMAPS
Radiation hardness
Upgrade

ABSTRACT

The increasing availability of commercial CMOS processes with high-resistivity wafers has fueled the R&D of depleted monolithic active pixel sensors (DMAPS) for use in high energy physics experiments. One of these developments is a series of monolithic pixel detectors with column-drain readout architecture and small collection electrode allowing for low-power designs (TJ-Monopix). It is designed in a 180 nm TowerJazz CMOS process and features a pixel size of $33 \mu\text{m} \times 33 \mu\text{m}$. The efforts and improvements on the front-end electronics and sensor design of the current iteration TJ-Monopix2 increase the radiation hardness and efficiency while lowering the threshold and noise.

1. Introduction

While monolithic active pixel sensors (MAPS) for particle physics experiments have been developed and tested since the 1990s [1,2], advances in CMOS technologies led to a new generation of MAPS by depleting the charge sensitive volume [3]. These depleted monolithic active pixel sensors (DMAPS) collect charges by drift in the depleted volume which offers faster readout times and higher radiation tolerance than MAPS. With increasing availability of high-resistivity silicon in commercial CMOS technologies the mentioned advantages of DMAPS can possibly be improved while profiting from the cheaper and faster production in commercial foundries. This makes DMAPS an interesting candidate for high-energy particle physics experiments with high particle rates in high radiation environments. One of the ongoing DMAPS development lines, TJ-Monopix, will be presented and evaluated in this article.

2. Design of DMAPS prototypes

The TJ-Monopix series of depleted monolithic active pixel sensors are designed in a commercial 180 nm CMOS process provided by Tower Semiconductor.¹ It is based on the ALPIDE pixel detector [4] for the

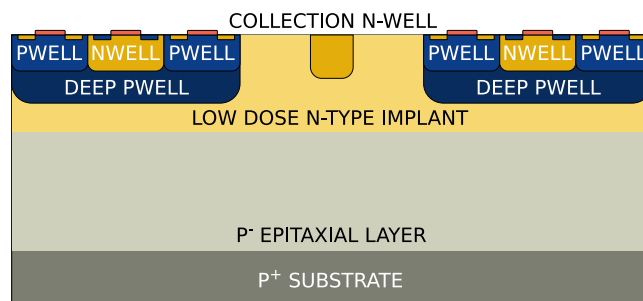


Fig. 1. Schematic cross-section of TJ-Monopix1 with a low-dose n-type silicon implant for a homogeneous electrical field and full depletion of the sensing volume (epitaxial layer).

ALICE ITS upgrade and a modification to the CMOS process to increase the radiation tolerance well beyond $10^{13} \text{ n}_{\text{eq}} \text{ cm}^{-2}$ [5]. With a small collection electrode of $2 \mu\text{m}$ the design offers a detector capacitance of only 3 fF [6]. The pixels are read out using an established synchronous column-drain mechanism developed for the FE-I3 readout chip [7].

* Corresponding author.

E-mail address: bespin@physik.uni-bonn.de (C. Bospin).

¹ <https://towersemi.com/>

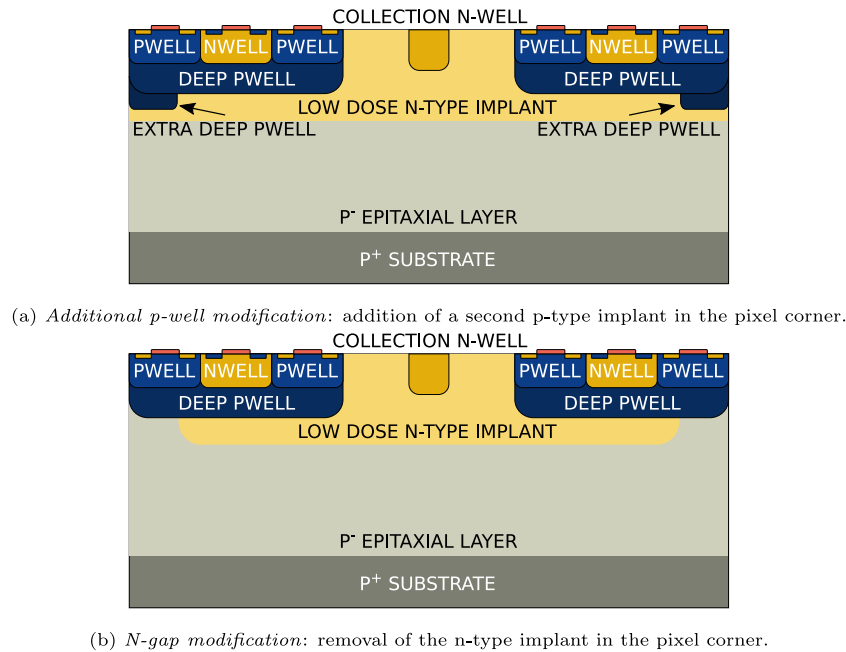


Fig. 2. Schematic cross-section of TJ-Monopix1 illustrating the modifications to the sensor to enhance the lateral electrical field in the pixel corners.

TJ-Monopix1. TJ-Monopix1 was the first iteration in this series of DMAPS featuring a pixel size of $36\ \mu\text{m} \times 40\ \mu\text{m}$ and a chip size of $2\ \text{cm} \times 1\ \text{cm}$. A schematic cross-section is shown in Fig. 1. The epitaxial layer as charge sensitive volume has a thickness of $25\ \mu\text{m}$. Sensors with $300\ \mu\text{m}$ thick sensitive volume were produced in a subsequent production run on Czochralski silicon wafers to investigate the performance with more charge produced in the sensor. In-pixel electronics are separated from the charge collection node and a deep p-well prevents n-type implants for electronics from forming a secondary charge collection node.

After an initial production run and subsequent tests, modifications to the sensor geometry shown in Fig. 2 were implemented and tested. Adding another p-well below the existing one or removing the n-type implant in the corners of the pixel results in a lateral electrical field in the regions below the in-pixel electronics. The motivations behind these changes will be discussed in Section 3.

TJ-Monopix2. As successor to TJ-Monopix1, TJ-Monopix2 implemented a series of changes following measurements on the former and a dedicated test chip Mini-MALTA in the same technology and with the same sensor design [8]. Besides the modifications to the sensor mentioned in the previous paragraph, the front-end electronics has been improved as well. Enlarging transistors in the analog front-end circuit is expected to reduce the threshold by a factor of 3 as well as improve threshold dispersion and noise behavior [9]. The scheme for masking individual pixels was also improved and a 3-bit DAC for local threshold adjustments in each pixel was added to further reduce the threshold dispersion.

The digital periphery of TJ-Monopix2 contains an integrated readout controller, LVDS drivers and receivers as well as the command decoder from the RD53B readout chip [10], which enables operation of the chip via four differential lines. Fig. 3 shows the digital chip architecture both in the pixel matrix and in the chip periphery.

3. Hit detection efficiency for TJ-Monopix1 prototype

Initial performance results for the first submission of TJ-Monopix1 prototypes have been reported [11,12]. Most notably, a significant loss

in hit detection efficiency ϵ_{Hit} in neutron irradiated devices has been observed, where the efficiency decreased from 97% before irradiation to 69% after irradiation to NIEL fluences of $1 \times 10^{15}\ \text{n}_{eq}\ \text{cm}^{-2}$.

Following simulations [13] and measurements on a test chip [8] implementing the proposed changes to the sensor, chips were produced in different variations of $30\ \mu\text{m}$ thick epitaxial layer and $300\ \mu\text{m}$ thick Czochralski silicon wafers with the sensor modifications presented in Fig. 2. The sensors produced on a thicker substrate instead of the epitaxial layer potentially offer larger charge signals produced in the depleted volume such that in cases of charge sharing in the pixel corners the partial charges can still pass the threshold. Neutron irradiated samples with the same fluence as in previous measurements were measured in a 5 GeV electron beam at the test beam facility at DESY [14].

A sensor built on epitaxial silicon with the n-gap modification is compared to a Czochralski silicon sensor with additional p-well, both of which are expected to perform significantly better than the initial sensor design with a continuous n-implant. Both investigated designs are biased by applying $-20\ \text{V}$ on the backside of the sensor and additional $30\ \text{V}$ on the collection electrode via a capacitor resulting in a total bias voltage of $50\ \text{V}$ across the sensor. The results for ϵ_{Hit} for each module are projected onto a 2×2 pixel array and depicted in Fig. 4.

With an efficiency of 87.1% for the $30\ \mu\text{m}$ thick sensor in Fig. 4(a) it can be confirmed that the sensor modifications account for a significant improvement of hit detection efficiency in irradiated sensors compared to the original process that achieved 69% at $1 \times 10^{15}\ \text{n}_{eq}\ \text{cm}^{-2}$. While the pixel center is even more efficient it can be seen that the efficiency losses occur in the corners of the pixels where charge sharing is more prominent. In the sensor built on Czochralski silicon, further improvements to the hit detection efficiency can be observed with more than 98% as depicted in Fig. 4(b). As the resistivity for both the epitaxial layer and the Czochralski silicon substrate are in the same order of $>1\ \text{k}\Omega\ \text{cm}$, the increased efficiency can be attributed to the larger sensitive volume. The depletion depth can be estimated from measuring the detected charge, which leads to approximately $45\ \mu\text{m}$ in the Cz silicon, an increase of 50% compared to the sensor with a $30\ \mu\text{m}$ thick epitaxial layer. While the pixel centers of the module

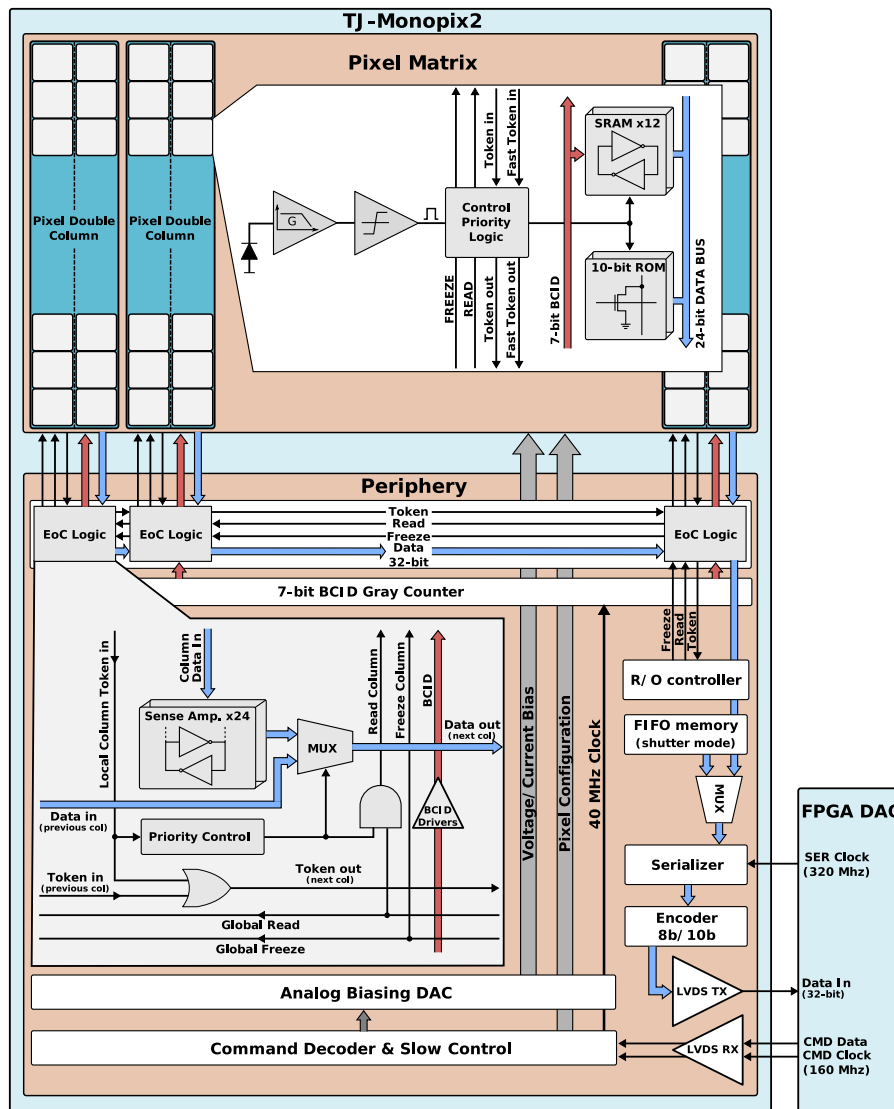


Fig. 3. Schematic overview of the digital logic in TJ-Monopix2 [9].

on Czochralski silicon show efficiencies above 99% there are losses in the pixel corners observable, but not as pronounced as in Fig. 4(a). From [13] it is expected to collect even more charge in a sensor with n-gap modification compared to the additional p-well modification, which could increase the efficiency in a thicker sensor to even more.

4. First measurement results for TJ-Monopix2

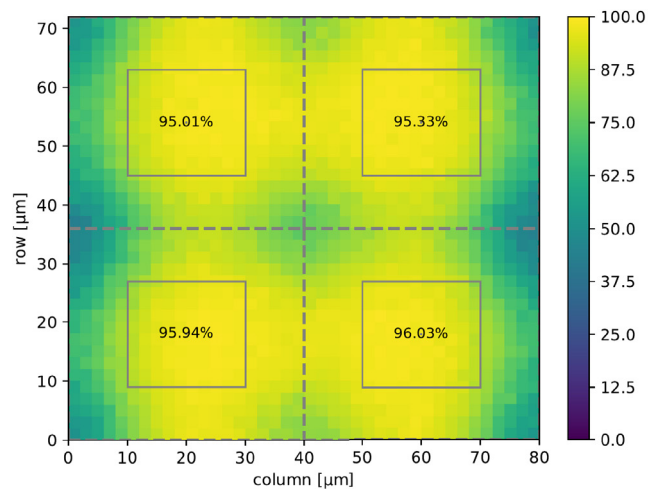
First tests show that the threshold in TJ-Monopix2 in the order of $100e^-$ is significantly lower than the previously measured values around $300e^-$ in TJ-Monopix1. The threshold distribution for an untuned chip without any optimizations is shown in Fig. 5(a). The local threshold DACs in the pixels are at the default value which yields a mean threshold of $153e^-$ and threshold dispersion $11e^-$ using a preliminary calibration with a radioactive ^{55}Fe source. To minimize the threshold variation between pixels in the matrix, the local threshold DACs in every pixel need to be tuned. By injecting 100 hits with the target threshold charge into each pixel the local DAC is adjusted such

that every pixel registers a number of hits as close as possible to 50. This is the expected number of detected hits at the threshold when sending 100 injection pulses. The resulting threshold distribution after this adjustment is presented in Fig. 5(b).

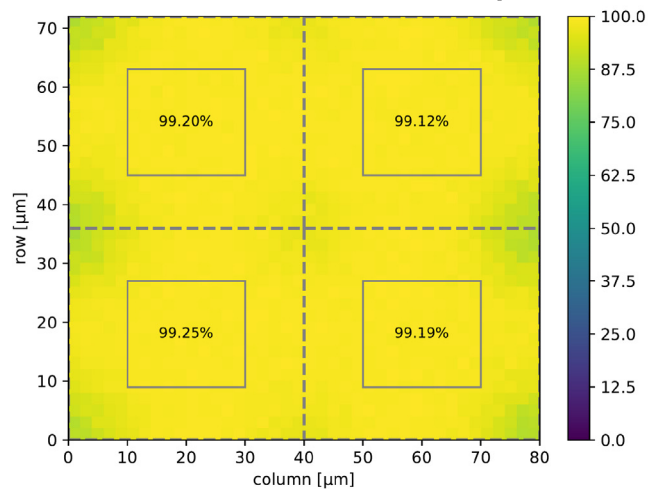
While the mean threshold is not improved ($156e^-$), as expected, the threshold dispersion could be halved to $5e^-$. Both numbers for the mean threshold and the threshold dispersion are an enhancement from TJ-Monopix1, and the front-end settings for the presented results are not yet optimized. With further adjustment of the settings the minimum achievable threshold could be even lower.

5. Conclusions

Measurements of neutron irradiated TJ-Monopix1 sensors with a modified sensor geometry have shown significant increase in hit detection efficiency. The sensor can be depleted to a depth of ca. $45\ \mu\text{m}$ leading to a higher collected charge in sensors thicker than the initial design with a $30\ \mu\text{m}$ epitaxial layer, which subsequently results in an



(a) Chip with 30 μm thick sensitive volume at $1 \times 10^{15} \text{ n}_{\text{eq}} \text{ cm}^{-2}$. $\epsilon_{Hit} = 87.1\%$



(b) Chip with 300 μm thick sensitive volume at $1 \times 10^{15} \text{ n}_{\text{eq}} \text{ cm}^{-2}$. $\epsilon_{Hit} = 98.6\%$

Fig. 4. Hit detection efficiency of (a) a chip with 30 μm thick epitaxial layer and n-gap sensor modification and (b) a chip with 300 μm thick sensitive volume in Czochralski silicon with extra p-well modification after irradiation. The figures depict information from all pixels folded into a 2×2 pixel array, where the dashed lines represent the pixel edges. The gray boxes are used to calculate $\epsilon_{Hit,center}$ in the pixel center for the respective pixel in the 2×2 grid.

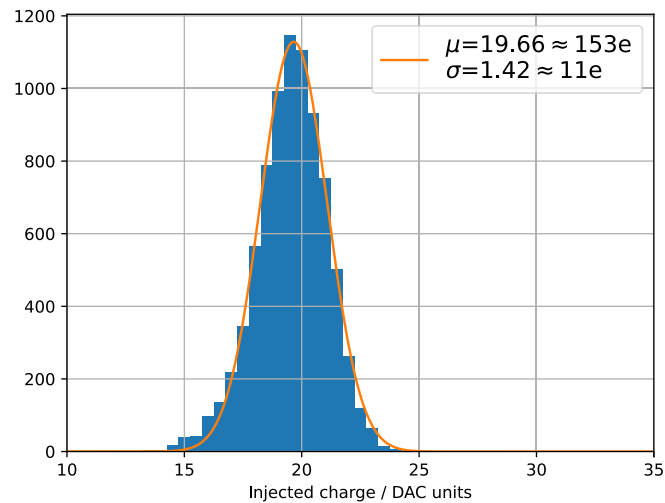
almost fully efficient pixel detector after neutron irradiation to $1 \times 10^{15} \text{ n}_{\text{eq}} \text{ cm}^{-2}$. In order to increase the efficiency after irradiation to higher values or increase the radiation tolerance to higher fluences, the signal charge needs to be increased as well. This can be achieved by larger depleted volume, either by higher voltage capabilities or silicon with higher resistivity, which both come at a cost of more required sensor volume. To keep the sensors as thin as possible (for example in experiments with predominantly light particles) it is necessary to lower the threshold in a way such that partial charges after charge sharing can still be measured. This improvement was done for TJ-Monopix2 which achieves thresholds of around $150 e^-$ or possibly lower. Furthermore, it was shown that the threshold dispersion could also be improved by an in-pixel threshold DAC, potentially allowing for even lower thresholds. With its specifications and expected performance, TJ-Monopix2 will serve as a prototype chip for a future DMAPS chip (OBELIX) that will be investigated for a potential future upgrade of the Belle II vertex detector at SuperKEKB.

Declaration of competing interest

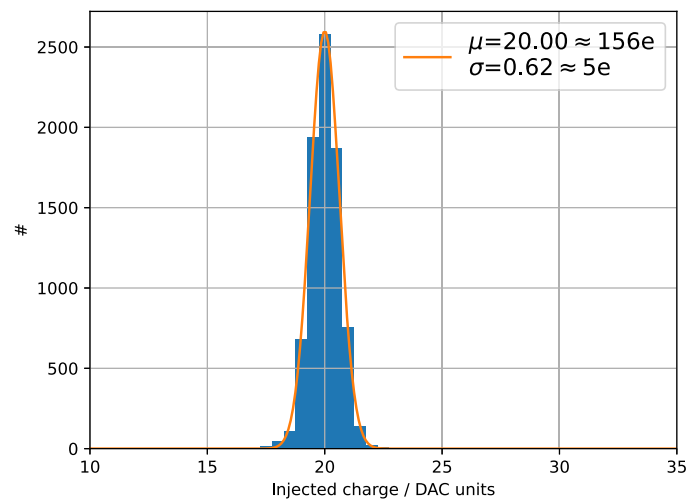
The authors declare that they have no known competing financial interests or personal relationships that could have appeared to influence the work reported in this paper.

Acknowledgment

This project has received funding from the Deutsche Forschungsgemeinschaft DFG, Germany (grant WE 976/4-1), the German Federal Ministry of Education and Research BMBF (grant 05H15PDCA9), and the European Union's Horizon 2020 research and innovation program under grant agreement no. 675587 (Maria Skłodowska-Curie ITN STREAM), 654168 (AIDA-2020), and 101004761 (AIDAInnova). The measurements leading to these results have been performed at the Test Beam Facility at DESY Hamburg (Germany), a member of the Helmholtz Association (HGF).



(a) Threshold distribution of an untuned TJ-Monopix2 chip.



(b) Threshold distribution of a tuned TJ-Monopix2 chip.

Fig. 5. Threshold distributions (a) before and (b) after optimizing the in-pixel threshold DACs in TJ-Monopix2 [15].

References

- [1] W. Snoeys, J. Plummer, G. Rosseel, C.H. Aw, C. Kenney, S. Parker, First beam test results from a monolithic silicon pixel detector, *Nucl. Instrum. Methods Phys. Res. A* 326 (1) (1993) 144–149, [http://dx.doi.org/10.1016/0168-9002\(93\)90344-H](http://dx.doi.org/10.1016/0168-9002(93)90344-H).
- [2] R. Turchetta, J. Berst, B. Casadei, G. Claus, C. Colledani, W. Dulinski, Y. Hu, D. Husson, J. Le Normand, J. Riestler, G. Deptuch, U. Goerlach, S. Higuere, M. Winter, A monolithic active pixel sensor for charged particle tracking and imaging using standard VLSI CMOS technology, *Nucl. Instrum. Methods Phys. Res. A* 458 (3) (2001) 677–689, [http://dx.doi.org/10.1016/S0168-9002\(00\)00893-7](http://dx.doi.org/10.1016/S0168-9002(00)00893-7).
- [3] I. Perić, A novel monolithic pixelated particle detector implemented in high-voltage CMOS technology, *Nucl. Instrum. Methods Phys. Res. A* 582 (3) (2007) 876–885, <http://dx.doi.org/10.1016/j.nima.2007.07.115>, VERTEX 2006.
- [4] M. Mager, ALPIDE, the monolithic active pixel sensor for the ALICE ITS upgrade, *Nucl. Instrum. Methods Phys. Res. A* 824 (2016) 434–438, <http://dx.doi.org/10.1016/j.nima.2015.09.057>.
- [5] W. Snoeys, G.A. Rinella, H. Hillemanns, T. Kugathasan, M. Mager, L. Musa, P. Riedler, F. Reidt, J.V. Hoorne, A. Fenigstein, T. Leitner, A process modification for CMOS monolithic active pixel sensors for enhanced depletion, timing performance and radiation tolerance, *Nucl. Instrum. Methods Phys. Res. A* 871 (2017) 90–96, <http://dx.doi.org/10.1016/j.nima.2017.07.046>.
- [6] K. Moustakas, M. Barbero, I. Berdalovic, C. Bepin, P. Breugnon, I. Caicedo, R. Cardella, Y. Degerli, N. Egidios Plaja, S. Godiot, F. Guilloux, T. Hemperek, T. Hirono, H. Krüger, T. Kugathasan, C. Marin Tobon, P. Pangaud, H. Pernegger, P. Riedler, P. Rymaszewski, E. Schioppa, W. Snoeys, M. Vandenbroucke, T. Wang, N. Wermes, CMOS monolithic pixel sensors based on the column-drain architecture for the HL-LHC upgrade, *Nucl. Instrum. Methods Phys. Res. A* 936 (2019) 604–607, <http://dx.doi.org/10.1016/j.nima.2018.09.100>, Frontier Detectors for Frontier Physics: 14th Pisa Meeting on Advanced Detectors.
- [7] I. Perić, L. Blanquart, G. Comes, P. Denes, K. Einsweiler, P. Fischer, E. Mandelli, G. Meddeler, The FEI3 readout chip for the ATLAS pixel detector, *Nucl. Instrum. Methods Phys. Res. A* 565 (1) (2006) 178–187, <http://dx.doi.org/10.1016/j.nima.2006.05.032>, Proceedings of the International Workshop on Semiconductor Pixel Detectors for Particles and Imaging.

- [8] M. Dyndal, V. Dao, P. Allport, I.A. Tortajada, M. Barbero, S. Bhat, D. Bortoletto, I. Berdalovic, C. Bepin, C. Buttar, I. Caicedo, R. Cardella, F. Dachs, Y. Degerli, H. Denizli, L.F.S. de Acedo, P. Freeman, L. Gonella, A. Habib, T. Hemperek, T. Hirono, B. Hiti, T. Kugathasan, I. Mandić, D. Maneuski, M. Mikuz, K. Moustakas, M. Munker, K. Oyulmaz, P. Pangaud, H. Pernegger, F. Piro, P. Riedler, H. Sandaker, E. Schioppa, P. Schwemling, A. Sharma, L.S. Argemi, C.S. Sanchez, W. Snoeys, T. Suligoi, T. Wang, N. Vermes, S. Worm, Mini-MALTA: radiation hard pixel designs for small-electrode monolithic CMOS sensors for the High Luminosity LHC, *J. Instrum.* 15 (02) (2020) P02005, <http://dx.doi.org/10.1088/1748-0221/15/02/p02005>.
- [9] K. Moustakas, Design and Development of Depleted Monolithic Active Pixel Sensors with Small Collection Electrode for High-Radiation Applications, (Ph.D. thesis), Rheinische Friedrich-Wilhelms-Universität Bonn, 2021, URL <https://hdl.handle.net/20.500.11811/9315>.
- [10] M. Garcia-Sciveres, F. Loddo, J. Christiansen, RD53 collaboration Collaboration, RD53B Manual, Tech. rep., CERN, Geneva, 2019, URL <https://cds.cern.ch/record/2665301>.
- [11] I. Caicedo, M. Barbero, P. Barrillon, I. Berdalovic, S. Bhat, C. Bepin, P. Breugnon, R. Cardella, Z. Chen, Y. Degerli, J. Dingfelder, S. Godiot, F. Guilloux, T. Hirono, T. Hemperek, F. Hügging, H. Krüger, T. Kugathasan, K. Moustakas, P. Pangaud, H. Pernegger, D.-L. Pohl, P. Riedler, A. Rozanov, P. Rymaszewski, P. Schwemling, W. Snoeys, M. Vandenbroucke, T. Wang, N. Vermes, The Monopix chips: depleted monolithic active pixel sensors with a column-drain read-out architecture for the ATLAS inner tracker upgrade, *J. Instrum.* 14 (06) (2019) C06006, <http://dx.doi.org/10.1088/1748-0221/14/06/c06006>.
- [12] C. Bepin, M. Barbero, P. Barrillon, I. Berdalovic, S. Bhat, P. Breugnon, I. Caicedo, R. Cardella, Z. Chen, Y. Degerli, J. Dingfelder, L. Flores Sanz de Acedo, S. Godiot, F. Guilloux, T. Hirono, T. Hemperek, F. Hügging, H. Krüger, T. Kugathasan, C. Marin Tobon, K. Moustakas, P. Pangaud, H. Pernegger, F. Piro, P. Riedler, A. Rozanov, P. Rymaszewski, P. Schwemling, W. Snoeys, M. Vandenbroucke, T. Wang, N. Vermes, S. Zhang, DMAPS monopix developments in large and small electrode designs, *Nucl. Instrum. Methods Phys. Res. A* 978 (2020) 164460, <http://dx.doi.org/10.1016/j.nima.2020.164460>.
- [13] M. Munker, M. Benoit, D. Dannheim, A. Fenigstein, T. Kugathasan, T. Leitner, H. Pernegger, P. Riedler, W. Snoeys, Simulations of CMOS pixel sensors with a small collection electrode, improved for a faster charge collection and increased radiation tolerance, *J. Instrum.* 14 (05) (2019) C05013, <http://dx.doi.org/10.1088/1748-0221/14/05/c05013>.
- [14] R. Diener, J. Dreyling-Eschweiler, H. Ehrlichmann, I. Gregor, U. Kötz, U. Krämer, N. Meyners, N. Potylitsina-Kube, A. Schütz, P. Schütze, M. Stanitzki, The DESY II test beam facility, *Nucl. Instrum. Methods Phys. Res. A* 922 (2019) 265–286, <http://dx.doi.org/10.1016/j.nima.2018.11.133>.
- [15] J. Dingfelder, M. Barbero, P. Barrillon, I. Berdalovic, C. Bepin, P. Breugnon, I. Caicedo, R. Cardella, Y. Degerli, L. Flores Sanz de Acedo, F. Guilloux, A. Habib, T. Hirono, T. Hemperek, F. Hügging, H. Krüger, T. Kugathasan, K. Moustakas, P. Pangaud, H. Pernegger, F. Piro, D.-L. Pohl, P. Riedler, A. Rozanov, P. Rymaszewski, P. Schwemling, W. Snoeys, T. Wang, N. Vermes, S. Zhang, Progress in DMAPS developments and first tests of the Monopix2 chips in 150 nm LFoundry and 180 nm TowerJazz technology, *Nucl. Instrum. Methods Phys. Res. A* 1034 (2022) 166747, <http://dx.doi.org/10.1016/j.nima.2022.166747>.